scientific reports

Check for updates

OPEN

Distinct astrocyte activation patterns associated with neuroinflammation induced by gamma and proton beam irradiation

Liben Yan[1,4], Tianyi Er[1,4], Shaoqian Sun[1]✉, Yulin Deng[1], Zhirong Wan[2], Jing Zhao[2], Ailu Wang[1], Beiqin Liu[1], Qiaojuan Wang[3], Li Sui[3]✉ & Hong Ma[1]✉

The aim of this study was to investigate the impact of radiation exposure on astrocyte response and assess their potential roles and mechanisms in surrounding neural cells. Healthy male rats were irradiated different radiation types to induce the neural inflammation. U87-MG cells were exposed respectively to gamma rays (2 Gy and 10 Gy) and proton irradiation (0.1 Gy and 0.5 Gy). Cell viability, mRNA expression, mitochondrial membrane potential, glucose uptake and cytokine levels were analyzed respectively to evaluate the neuroinflammation or neural damage. Gamma rays and proton beam irradiation induced distinct patterns of inflammatory factor expression in the hippocampal region of rats. Moreover, we observed changes in cell morphology and a dose-dependent inhibition of cell proliferation across all radiation types. Significant upregulation of caspase-8 and caspase-3 enzymatic activities in U87-MG cells was observed after exposure to gamma rays. Astrocytes showed increased expression of GFAP, C3, and PTX3 after exposure to gamma rays, and downregulation while exposure to proton. Additionally, proton beam irradiation potentially increased glutamine synthesis in astrocytes. Furthermore, we investigated the influence of irradiated astrocytes on neurons via mitochondrial integrity, neurotransmitter levels, and glucose metabolism. Additionally, the expression of miR92a-3p, which can significantly downregulate GFAP and IL-6 expression, was downregulated by gamma rays, while upregulated by proton irradiation. The findings highlight the differential impact of gamma rays and proton radiation on inflammatory responses in vivo, with gamma rays inducing a pro-inflammatory effect and proton radiation exerting anti-inflammatory properties. Overall, this study provides valuable insights for radiotherapy management.

Keywords Astrocytes, Neuroinflammation, Radiotherapy, microRNA

Abbreviations

RBI	Radiation-induced brain injury
TME	Tumor microenvironment
CNS	Nervous system

Radiotherapy is the first-line treatment for primary and metastatic brain tumors[1]. However, normal brain tissue surrounding the tumor is inevitably included in the radiation affected area, leading to the occurrence of radiation-induced brain injury (RBI). RBI is a common complication in cancer patients after radiotherapy, and it is often irreversible, seriously affecting the prognosis and quality of life of patients[2,3]. The molecular and cellular mechanisms of RBI are extremely complex, and our understanding of the damage mechanisms of RBI at the cellular and molecular levels is still limited. However, previous research results have shown that the radiation-induced brain tissue damage effect is an extremely complex dynamic interaction between multiple types of

[1]School of Medical Technology, Beijing Institute of Technology, Beijing 100081, China. [2]Department of Neurology, Aerospace Center Hospital, Beijing, China. [3]Department of Nuclear Physics, China Institute of Atomic Energy, Beijing 100081, China. [4]Liben Yan and Tianyi Er contributed equally to this work. ✉email: 7520220011@bit.edu.cn; lisui@ciae.ac.cn; 04656@bit.edu.cn

cells in tumor microenvironment (TME), including glial cells, endothelial cells, and neurons. The damage of these cells initiates an inflammatory cascade reaction and leads to progressive brain damage[4,5].The potential impact of RBI and TME on various biological processes, particularly the proinflammatory effects and the immune suppressive effects that can either promote or impede antitumor immunity has garnered increasing interest[6–8]. Previous research has revealed that radiation is associated with the promotion of oxidative stress and DNA damage[9–11]. These cellular responses are closely interconnected with the activation of pro-inflammatory signaling cascades, prompting the release of cytokines, chemokines, and other mediators of inflammation. Studies examining the biological effects of radiation have disclosed that radiation exposure induces the activation of inflammasome[11,12]. Upon exposure to a certain dose of radiation, significant morphological changes occur in the subcortical and brainstem regions[13]. It has also been indicated that neuronal exposure to gamma radiation results in the activation and polarization of astrocytes, leading to oxidative and inflammatory damage in neurons[14]. These above investigations have indicated that radiation potentially precipitates the onset or progression of neuroinflammatory disorders and potential neuronal damage. Nevertheless, the impact of radiation related RBI on the nervous system (CNS) remains incompletely understood.

Astrocytes and microglia are the predominant non-neuronal cell types in the central nervous system, with crucial roles in supporting neuronal function and responding to various stimuli, including inflammation. There is growing evidence that radiation can engender the proliferation of microglial cells and astrocytes within the brain, culminating in a series of pro-inflammatory and chemotactic factors[15]. Moreover, radiation damages the nervous system by inhibiting development and causing functional impairments in neurons and supporting cells[13,16]. Understanding the dynamic interplay between glial cells and neurons is crucial for devising effective strategies to alleviate neuroinflammatory damage induced by radiation. While current research on the inflammatory response in radiotherapy conditions has predominantly examined the cellular level, our study focuses on investigating the specific and chronic inflammatory reactions occurring in the hippocampal region of rats after different exposure. Intriguingly, we have observed contrasting inflammatory responses elicited by ionizing radiation and particle radiation, emphasizing the necessity for further exploration into the underlying mechanisms governing these divergent reactions.

In this study, we focused on investigating the divergent changes in astrocytes under distinct radiation conditions, along with the ensuing neuroinflammatory consequences of such exposure. By evaluating a spectrum of biological effects and quantifying levels of inflammatory factors, we sought to dissect the intricate mechanisms underlying astrocytic responses to radiation. Interestingly, our investigations revealed a remarkable consistency between the responses observed at the cellular and organismal levels. This alignment suggested a coordinated interplay between radiation exposure, astrocytic function, and inflammatory, furnishing valuable insights into the distinct effects of diverse radiation sources on neuronal immune microenvironment.

Methods

Animal experiment

Rats and ethical statement

Healthy male SD (Sprague–Dawley) rats weighing 200 ± 20 g purchased from Beijing Sibeifu Biotechnology Co., Ltd., (SCXK (Jing) 2016-0002) and were cared for according to the "Guidelines for the Care and Use of Laboratory Animals." They were allowed 1–2 days of acclimatization before the experiments were conducted. All animal procedures were approved by the Animal Research Committee of Beijing Institute of Technology.

Radiation treatment for rats

In accordance with ethical standards, the experimental rats underwent environmental adaptation and stabilization before radiation exposure. The rats were divided into two groups: control, and radiation model groups, with 6 rats in each group. Two types of radiation sources were used in this experiment: Cobalt-60 (Co-60) γ-rays at a dose rate of 1 Gy/min for whole-body irradiation, with a cumulative dose of 4 Gy (Beijing Normal University Radiation Center, Beijing); and a proton animal radiation model, using protons from a cyclotron accelerator (100 MeV, 0.8 keV/μm) at a dose rate of 1 Gy/min for whole-body irradiation, with a cumulative dose of 1 Gy (China Institute of Atomic Energy, Beijing). Systematic observation and recording of the rats' mental status, survival rate, body weight, food and water intake, excretion were conducted at predetermined intervals to assess the rats' health status and the accuracy of the experimental model.

Tissue preparation

For observation of neuronal damage, on the 21st day, all groups were deeply anesthetized using isoflurane through a RWD gas anesthesia machine. With surgical scissors, the chest cavity was opened, and the diaphragm was cut to expose the animal's heart. An injection needle was inserted into the left ventricle, and the right atrial appendage was incised to create an outlet for blood and saline replacement, followed by the infusion of physiological saline. The absence of red fluid at the injury site of the right atrial appendage, along with the whitening of the rat's eyes and liver, indicated success. The needle was then removed, and the entire brain was extracted. The excised brain was then immersed in 4% paraformaldehyde for a fixation period exceeding 72 h.

Paraffin sectioning

The samples underwent gradient dehydration using 50%, 70%, 80%, 95%, and 100% ethanol, with each concentration lasting approximately 30 min. Xylene was added in equal volume to ethanol, followed by pure xylene to prevent tissue shrinkage and hardening. Complete dehydration was achieved when the tissues appeared transparent. A small amount of melted paraffin was added to embedding boxes, and the tissue blocks were placed inside, completely submerging them. The blocks were swiftly transferred to a cooling platform for sectioning. In this experiment, the hippocampal region of the brain tissue was sectioned to a thickness of 4 μm.

The paraffin sections were then placed on glass slides, dried, and baked at 60 °C for 2–4 h or at 37 °C overnight before being stored at room temperature.

Immunofluorescence staining

Paraffin-embedded tissue sections were deparaffinized with xylene three times, followed by rehydration with 100%, 95%, and 70% ethanol, and then incubated in distilled water to remove ethanol. The tissue sections were then subjected to antigen retrieval in EDTA antigen retrieval buffer (pH 8.0) in a steamer at 95 °C for 30 min. Next, the sections were immersed in 3% hydrogen peroxide solution at room temperature for 10 min. Subsequently, the sections were circled with a hydrophobic barrier pen, and then incubated with a self-quenching autofluorescence eliminator for 5 min. The sections were then incubated with the primary antibody for GFAP (Abcam ab53554), Iba1(Wako 019-19741), NeuN(Abcam ab104224) and overnight incubation at 4 °C. After washing with PBS for 3 times, the sections were incubated with the corresponding secondary antibody at room temperature for 1 h. Finally, the sections were mounted with anti-fade mounting reagent and subjected to panoramic scanning.

Cell lines and cell culture

The SH-SY5Y neuronal cell line (referred to as SH cells hereafter) and the U87-MG astrocytic cell line were procured from the Cell Center of the Chinese Academy of Medical Sciences. SH cells were cultured in DMEM/F12 medium (Gibco) supplemented with 10% fetal bovine serum (Gibco), 1 × penicillin–streptomycin, 1 × GlutaMAX (Gibco), 1 × sodium pyruvate, and 1 × non-essential amino acids (Gibco). U87-MG cells were cultured in DMEM medium supplemented with 10% fetal bovine serum, 1 × penicillin–streptomycin, and 1 × non-essential amino acids (Solarbio). All cells were maintained in a fully humidified incubator with 5% CO_2 at 37 °C.

Establishment of irradiation model and cell co-culture model

U87-MG cells were subjected to two types of radiation, including gamma rays and proton beam. The gamma ray irradiation was performed at the "Key Laboratory of Beam Technology" of the School of Nuclear Science and Technology, Beijing Normal University (Beijing Radiation Center), while proton radiation was tested at the Center for Innovative Applications of Anti-radiation Technology of the National Institute of Atomic Energy Agency. For the gamma ray and proton irradiation, U87-MG cells were plated at 4.5×10^5 cells per T25 culture flask with complete growth medium. After 8–10 h of incubation, the cells were fully adhered, and at normal atmospheric pressure and temperature, they were exposed to a total dose of 0.1–16 Gy of radiation at a dose rate of 1–2 Gy/min, as per the experimental protocols for different radiation types. Similarly, for proton irradiation, U87-MG cells were seeded at 4.5×10^5 cells per dish with complete growth medium, incubated for 8–10 h, and then exposed to a total dose of 0.2–2 Gy of proton radiation at a dose rate of 0.1 Gy/min under normal atmospheric conditions with the dishes sealed.

Before culturing under different conditions, SH cells were plated at 1×10^5 cells per well in a six-well culture plate with 2 mL of complete growth medium. After incubation, the conditioned media were collected 48 h after radiation and 24 h after conditioned culturing, centrifuged at 2000 rpm/min for 5 min, and stored at − 80 °C.

Subsequently, the cells were rinsed with sterile PBS, digested with trypsin, centrifuged, and then collected. 1 mL of Trizol and 1 mL of Ripa were added to each group of cells, labeled, and stored in a − 80 °C freezer for further analysis.

MTS assay

To measure cell viability, a mixture of 20 µL MTS and PMS solution (MTS: PMS = 20:1) was added to 100 µL of cells (5000–10,000 cells) per well in a 96-well culture plate, with 3–5 replicate wells per group. Subsequently, the 96-well culture plate was then placed in a cell culture incubator at 37 °C and 5% CO_2 for 1–4 h. The optical density (OD) value was then measured at 490 nm using a microplate reader. The OD values of the test wells were subtracted from the OD values of the control wells or blank wells, and the average OD value of the replicate wells was calculated. Cell viability was evaluated based on the OD values.

RNA extraction and RT-PCR

To extract RNA from the sample, 0.2 ml of chloroform was added and shaken for 15 s, followed by incubation at room temperature for 2–3 min, and centrifugation at 4 °C for 15 min. The RNA was precipitated by adding 0.5 ml isopropanol, and then washed in at least 1 ml of 75% ethanol. After discarding the supernatant, 20–30 µL of DEPC water was added to precipitate the RNA solution, which was stored in a − 80 °C freezer.

The RNA concentration was determined using a spectrophotometer with 1 µL of the sample. Then, 1 µL of Primer Oligo DT was added to 4 µg of RNA sample with a total volume of 5 µL. The initial reaction product (5 µL) was mixed with 15 µL reaction system and vortexed thoroughly. The cDNA was synthesized using a reverse transcription PCR (RT-PCR) system. PCR was performed using a two-step method with SYBR Green Premix for cDNA amplification. The pre-denaturation program consisted of 95 °C for 30 s, followed by a 40-cycle PCR reaction program of 95 °C for 5 s and 60 °C for 30 s. The melting curve program included steps at 95 °C for 60 s, 60 °C for 15 s, and 95 °C for 5 s. The relative expression level of the target gene was calculated using GAPDH as an internal reference, by the $2^{-\Delta\Delta Ct}$ method. The primer sequences are listed as follows:

GAPDH(Forward): GACTTCAACAGCAACTCCCACTCTTCC;
GAPDH(Reverse): TGGGTGGTCCAGGGTTTCTTACTCCTT;
IL-6(Forward): ACTCACCTCTTCAGAACGAATTG;
IL-6(Reverse): CCATCTTTGGAAGGTTCAGGTTG;
TNF-α(Forward): CCTCTCTCTAATCAGCCCTCTG;

TNF-α(Reverse): GAGGACCTGGGAGTAGATGAG.
C3(Forward): GGGGAGTCCCATGTACTCTATC.
C3(Reverse): GGAAGTCGTGGACAGTAACAG.
PTX3(Forward): CATCTCCTTGCGATTCTGTTTTGCCATTCCGAGTGCTCCTGA.
PTX3 (Reverse): AGGTCCATGTGGAGCTTGAC.
GFAP(Forward): AGGTCCATGTGGAGCTTGAC.
GFAP(Reverse): GCCATTGCCTCATACTGCGT.

Enzyme-linked immunosorbent assay (ELISA)

ELISA kits (FM-1588A, FM-1735A, FM-1721A, and FM-1731A, Business Department of Beijing Hanke Hengyu Biotechnology Co., Ltd) were used to detect the cytokines, as well as Glutamine (Gln) and Dopamine (DA). To prepare the corresponding standard curve, 50 μL of different concentrations of standard samples were added to each well, and blank wells (with a concentration of 0 standard sample, served as the negative control) were set up. Next, 10 μL of the test sample and 40 μL of sample diluent were added to the wells of the test sample. In the wells containing the standard samples and the test samples, 100 μL of horseradish peroxidase (HRP) labeled detection antibody was added. The plate was sealed with a plate sealer and incubated at 37 °C for 60 min. After that, each well was filled with wash buffer, left for 1 min, and then tapped dry on absorbent paper for 5 times. Subsequently, 50 μL of substrate A and B were added to each reaction well, and the plate was incubated at 37 °C for 15 min. Finally, 50 μL of stop solution was added to each well, and the absorbance at 450 nm was measured within 15 min.

Mitochondrial membrane potential detection

Cells were cultured in 6-well plates, washed 3 times with PBS, 1 ml of cell culture medium and 1 ml of JC-1 staining solution were added, and mixed thoroughly. Incubate at 37 °C for 20 min in a cell culture incubator. Wash 2 times with JC-1 staining buffer. Add 2 ml of cell culture medium, observe under a fluorescence microscope or laser confocal microscope, and set the excitation wavelength to 525 nm and the emission wavelength to 590 nm.

Glucose uptake assay

Initially, 1 mg of 2-NBDG was diluted in 2.92 mL of ddH_2O and further diluted in pre-warmed serum-free cell culture medium to prepare a 100 μM working solution of 2-NBDG. The cells were then cultured in a 6-well plate, washed three times with PBS, and subjected to a 20-min incubation at 37 °C with the 100 μM 2-NBDG working solution, followed by another round of PBS washing. Subsequently, three random regions from each well were observed under a fluorescence microscope, and the experiment was repeated three times. The average fluorescence intensity was calculated using Image J.

Transfection of miRNA mimics

The miRNA mimics were centrifuged for 1 min and resuspended in 50 μL of DEPC water to achieve a final concentration of 20 μM/μL. Subsequently, 2×10^4 cells were seeded in a 6-well plate and incubated for 12 h. Omifection-R transfection reagent was added to the miRNA mimic mixture, gently mixed, and left at room temperature for 30 min. The transfection complex was then added to the cell culture medium and incubated further. After 24–36 h post-transfection, the expression levels of the target gene miRNA were detected using qPCR to assess the success of transfection. The miRNA mimics (Mir-25-3p: CAUUGCACUUGUCUCGGUCUGA; mir-92-a-3-p: UAUUGCACUUGUCCCGGCCUGU; Mir-26a-5p used in this study: UUCAAGUAAUCCAGGAUAGGCU) were synthesized by Shanghai Sangon Biotechnology (Shanghai, China).

Statistical data analysis

In this study, data analysis was conducted using GraphPad Prism (Version 7.00). Standard deviations were represented in the form of error bars (± s). Significance analysis between groups was performed using one-way analysis of variance (ANOVA). The symbol * represented a p-value of less than 0.05. In all experiments with provided significance analysis, the number of replicates (n) was equal to or greater than 3.

Statement

All methods were performed in accordance with the ARRIVE guidelines.

Results

Impacts of gamma and proton radiation on inflammatory response in vivo

According to previous reports[17], we successfully established a whole-body irradiation induced neuroinflammation rat model. The survival rate, body weight, and liver index of rats were analyzed. The results showed that 1 Gy of proton and 4 Gy of gamma ray was the safe dose. At this time, there is no significant impact on the life and physiological status of the test animals. In the preliminary experiments, animals died when the gamma radiation was greater than 4 Gy, and when the proton radiation was greater than 1 Gy, animals died. Because we need to observe the chronic inflammatory response in the animal's body. Therefore, we want to keep the animal alive, and excessive doses can affect survival rates. So, 4 Gy gamma radiation and 1 Gy proton beam were selected.

It has been observed that both gamma ray and proton beam did not affect the body weight and brain weight of rats (Fig. 1A), suggesting that the radiation models did not cause harm to the animals, which could be utilized for further investigation. To explore the effects of radiation on the inflammatory response in vivo, we examined the levels of inflammatory factors in the hippocampal region of rats for 21 days after exposure. The results revealed that 4 Gy gamma rays significantly increased the expression of IL-1β, IL-6, IL-8, and TNF-α (Fig. 1C). Proton beam irradiation led to a notable increase in IL-6 expression, while reducing the levels of IL-8, with no effect on

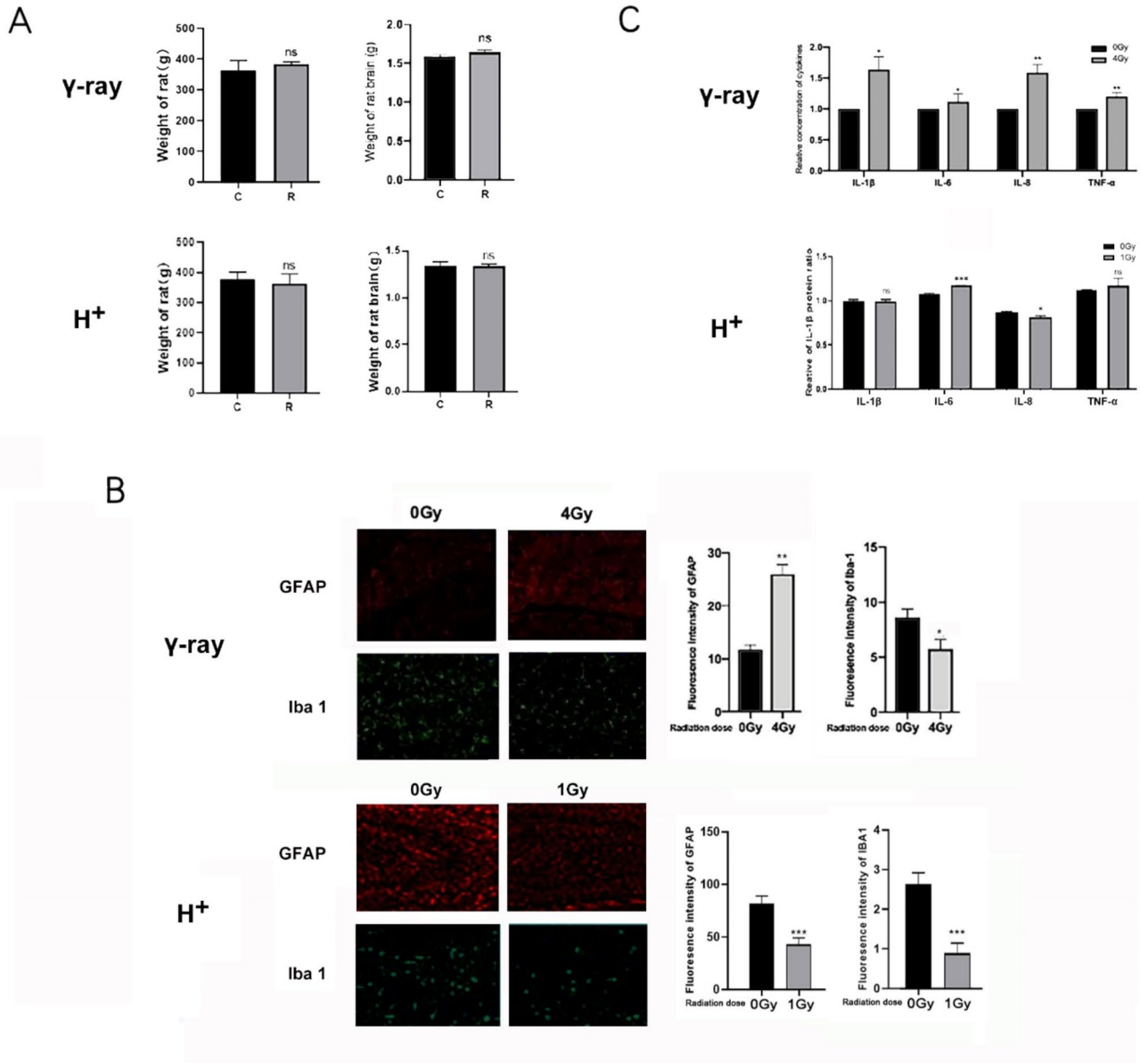

Fig. 1. Impact of gamma and proton radiation on the hippocampal inflammatory response in rats. (**A**) Body weight and brain weight of rats exposed to gamma and proton beam irradiation, respectively. (**B**) Immunofluorescence staining of Iba-1 and GFAP in the hippocampal region after gamma and proton beam irradiation, respectively. (**C**) Expression levels of IL-1β, IL-6, IL-8, and TNF-α in the hippocampal region after gamma and proton beam irradiation, respectively. $^{*}P<0.05$, $^{**}P<0.01$, $^{***}P<0.001$. γ-ray: gamma irradiation; H^{+}: proton beam irradiation.

IL-1β and TNF-α levels (Fig. 1C). Moreover, we thoroughly evaluated the key features of neuroinflammation, including the activation of microglia and astrocytes. 4 Gy gamma rays significantly elevated the expression levels of glial fibrillary acidic protein (GFAP) and Iba1 (Fig. 1B). Additionally, proton beam irradiation significantly reduced GFAP and Iba1 expression levels (Fig. 1B). These results implied differential impact of gamma rays and proton radiation on the inflammatory response in the hippocampal region of rats, with gamma rays inducing a pro-inflammatory effect and proton radiation exerts some anti-inflammatory properties.

Impact of astrocyte cell viability by two types of radiation

In order to further clarify the differential mechanisms of neuroinflammation related to astrocytes induced by different radiation, we established an activation model of astrocytes induced by gamma ray and proton beam in vitro. The experiment selects two different doses for the functional study of astrocytes: the tolerated dose with a cell survival rate of about 80% after 48 h of irradiation and the half lethal dose with a cell survival rate of about 50%. When the gamma ray irradiation dose was 2 Gy and 10 Gy, the cell proliferation rate decreased to 81% and 51% compared to the control group; When the proton beam irradiation dose was 0.1 Gy and 0.5 Gy,

the cell proliferation rate decreased to 79% and 53% compared to the control group; Therefore, the gamma ray irradiation doses were selected as 2 Gy and 10 Gy; Proton beam irradiation doses of 0.1 Gy and 0.5 Gy were selected.

We first evaluated the effects of radiation on the viability of astrocyte, and determined the changes in cell morphology and proliferation of U87-MG following exposure to gamma rays and proton beams. As shown as Fig. 2, following exposure to the two types and doses of radiation, the U87-MG cells exhibited a transformation in cell morphology from spindle-shaped to irregular, accompanied by elongation of the cells (Fig. 2A). Subsequently, we found the proliferation levels of the cells were significantly inhibited after irradiation with each type of radiation. Comparing with the control group, the cell proliferation rates decreased to 81% and 51% for 2 Gy and 10 Gy gamma ray irradiation, while 79% and 53% for 0.1 Gy and 0.5 Gy proton beam irradiation (Fig. 2B). These findings indicated a clear dose-dependent effect, with higher doses resulting in stronger inhibition of cell proliferation across all radiation types.

In order to investigate the potential induction of apoptosis in astrocytes by radiation exposure, we evaluated the activation of caspase-8 and caspase-3 in U87-MG cells following exposure to different radiation sources. It was found that the enzymatic activities of caspase-8 and caspase-3 in U87-MG cells were significantly upregulated after exposure to gamma rays (Fig. 2C), with the increase in activity proportional to the dose, indicating the potential occurrence of apoptosis in cells irradiated to gamma rays. In comparison to the control group, U87-MG cells irradiated with proton beams showed no significant difference in caspase-8 activity (Fig. 2D). However, under the tolerance dose (0.1 Gy) irradiation condition, caspase-3 activity was significantly decreased compared to the control group. Under the half-lethal dose (0.5 Gy) irradiation, there was no significant difference compared to the control group, but a significant increase was observed compared to 0.1 Gy. These findings indicated the potential differential impact of two types of radiation on the apoptosis related signal molecule of astrocytes. Gamma rays can induce caspase dependent cell apoptosis, but the inhibition of cell proliferation caused by proton irradiation is not closely related to caspase signaling molecules.

Impact of radiation on astrocyte activation and glutamine levels

After being stimulated by external factors, the central nervous system may develop neuroinflammation, which is mainly manifested by the activation and polarization of astrocytes, Glial fibrillary acidic protein (GFAP) is one of the main skeletal proteins of astrocytes and is also recognized as a characteristic marker of astrocytes. After the activation of astrocytes, they are called reactive astrocytes. Reactive astrocytes undergo polarization and are mainly divided into two types: A1 phenotype and A2 phenotype. A1 reactive astrocytes produce pro-

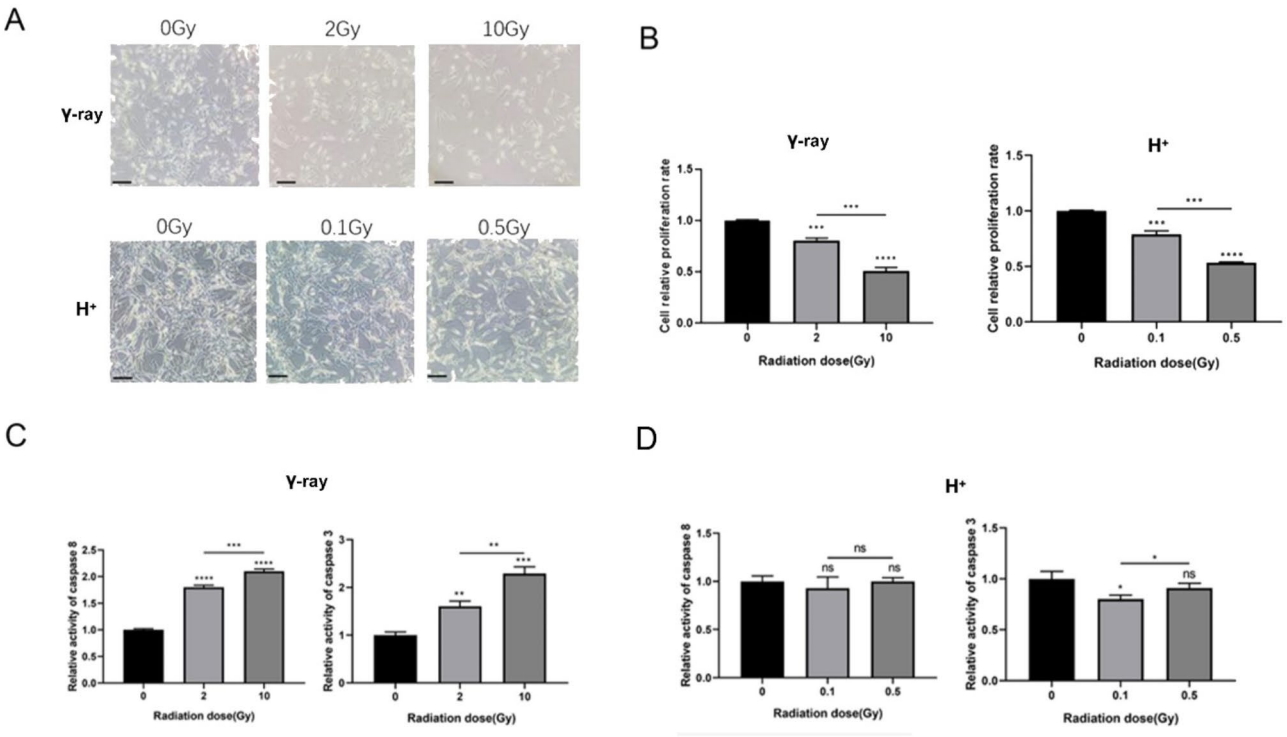

Fig. 2. Impact of different radiation doses and types on the cell viability of astrocytes. (**A**) Morphological changes of U87-MG cells exposed to different dose of gamma (2 Gy and 10 Gy) and proton beam (0.1 Gy and 0.5 Gy) irradiation, respectively. (**B**) Cell proliferation rate of U87-MG cells after gamma and proton beam irradiation, respectively. (**C**) Caspase-3 and caspase-8 activity in U87-MG cells after different dose of gamma irradiation. (**D**) Caspase-3 and caspase-8 activity in U87-MG cells after different dose of proton beam irradiation. $^{*}P<0.05$, $^{**}P<0.01$, $^{***}P<0.001$. γ-ray: gamma irradiation; H^{+}: proton beam irradiation.

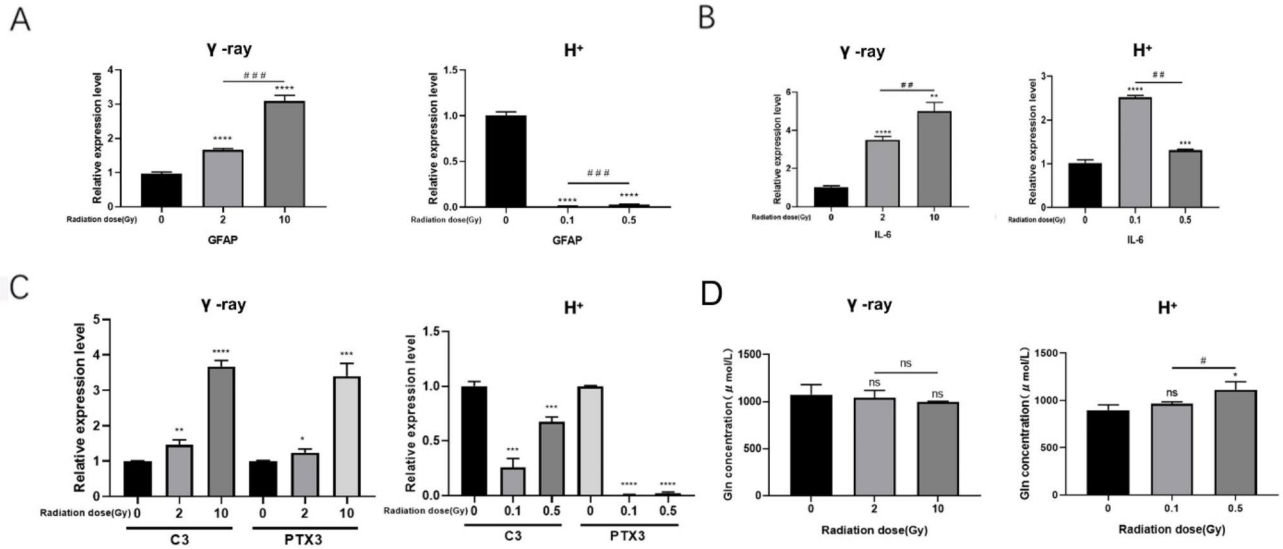

Fig. 3. Impact of different radiation doses and types on astrocyte activation, inflammatory response and glutamine levels. (**A**, **B**) Expression levels of GFAP and IL-6 in U87-MG cells after different dose of gamma and proton beam irradiation, respectively. (**C**) Expression levels of C3 and PTX3 in U87-MG cells after different dose of gamma and proton beam irradiation, respectively. (**D**) Glutamine levels in U87-MG cells after different dose of gamma and proton beam irradiation, respectively. $^{*}P<0.05$, $^{**}P<0.01$, $^{***}P<0.001$. γ-ray: gamma irradiation; H^{+}: proton beam irradiation; Gln: glutamine.

Ray type and characteristic			Inhibit cell proliferation	Apoptosis Associated enzyme activity	Cell activation	Cell polarization	Glutamine synthesis
γ-ray	Hertzian waves	Low LET low energy	+	↑	↑	↑	−↓
H +	Particulate	Low LET medium energy	+	↓	↓	↓	−↑

Table 1. Astrocyte damage caused by different radiation irradiation at tolerated doses. +: Present, −: No change, ↑: Enhanced, ↓: Decreased, −↑: Enhanced but not significant, −↓: Decreased but not significant.

inflammatory factors, causing damage to neurons; A2 reactive astrocytes provide nutritional support and secrete factors that regulate inflammatory responses, promoting neuronal survival and repair. Therefore, in this paper, GFAP gene was chosen as the marker for activation of astrocytes, while C3 gene was selected as the marker for A1 polarization of reactive astrocytes; The PTX3 gene is selected as a marker for A2 polarization in reactive astrocytes.

In order to examine the impact of different radiation sources on the activation of astrocytes, we analyzed the gene expression levels of GFAP, IL-6, C3, and PTX3 in U87-MG cells after exposure to gamma-ray and proton irradiation. We observed an upregulation of GFAP gene expression following gamma-ray irradiation (Fig. 3A). In contrast, proton beam radiation led to a significant downregulation of GFAP expression at both tolerable and semi-lethal doses, indicative of astrocyte activation (Fig. 3A). The expression of IL-6 levels was significantly upregulated by gamma-ray and proton irradiation (Fig. 3B). This is consistent with the results of our rat model. Furthermore, a significant and dose-dependent upregulation of both C3 and PTX3 gene expression in astrocytes was observed following gamma-ray irradiation (Fig. 3C). While proton irradiation led to significant downregulation of C3 and PTX3 gene expression, with a degree of recovery at the semi-lethal dose observed in C3 expression (Fig. 3C). In conclusion, the findings demonstrated that the alterations of GFAP and IL-6 were consistent between in vitro cell models and in vivo models, further highlighting the distinct effects of two types of radiation on astrocyte activation and inflammatory activity.

Impaired glutamate uptake by astrocytes can lead to neuronal excitatory toxicity, which is usually associated with neurodegenerative diseases[18]. With the aim of investigating whether different radiation sources might induce excitatory neurotoxic effects on astrocytes, this study conducted an analysis of glutamine content in U87-MG cells. As illustrated in Fig. 3D, irrespective of gamma-ray exposure, there were no significant differences in glutamine content in astrocytes compared to the control group at tolerance and half-lethal doses. Following proton irradiation, the glutamine content in astrocytes showed no significant difference at the tolerance dose compared to the control group, yet exhibited a significant elevation at the half-lethal dose (Fig. 3D, right lane). We have summarized the different biological effects on astrocytes under gamma-ray radiation and proton particle radiation (Table 1). Overall, these findings suggested the differential impact of various radiation sources

on astrocytes, and then compared with gamma irradiation, proton irradiation might regulate nerve damage by reducing neuroinflammatory levels and enhancing glutamate uptake.

Effects of radiated astrocytes on neuronal function

To evaluate whether the differential response of astrocytes has a differential effect on neuronal function, we analyzed the changes in the number of mature neurons in the hippocampus region of the in vivo model. The results showed that the expression level of neuron specific nuclear protein (NeuN) increased in the gamma ray irradiation group, but decreased in the proton irradiation group (Fig. 4A). To give further investigation of the impact of irradiated astrocytes on neurons, we cultured neurons for 24 h in a medium of astrocytes that had been irradiated by radiation exposure. Briefly, neurons were cultured for 24 h in the conditioned medium of irradiated astrocytes, with a cell survival rate of approximately 80% maintained 48 h post-irradiation. Microscopic examination revealed no significant morphological changes in SH-SY5Y cells following irradiation with 2 Gy gamma rays and 0.1 Gy proton irradiation (Fig. 4B). To explore the influence of irradiated astrocytes on neuronal activity, we evaluated neuronal proliferation and apoptosis after culturing neurons in the conditioned medium of irradiated astrocytes. We found that following tolerable dose irradiation, both gamma rays and proton beams did not significantly affect neuronal proliferation compared to the control group (Fig. 4B). Furthermore, when SH-SY5Y neurons were cultured in the conditioned medium of irradiated astrocytes, the enzymatic activity of caspase-8 and caspase-3 was significantly upregulated compared to the control group following gamma and proton beam irradiation (Fig. 4C).

Next, we examined the mitochondrial membrane potential in conditioned SH-SY5Y cells post irradiation, to assess the impact of post-irradiation astrocytes on neuronal mitochondria. As depicted in Fig. 4D, post-

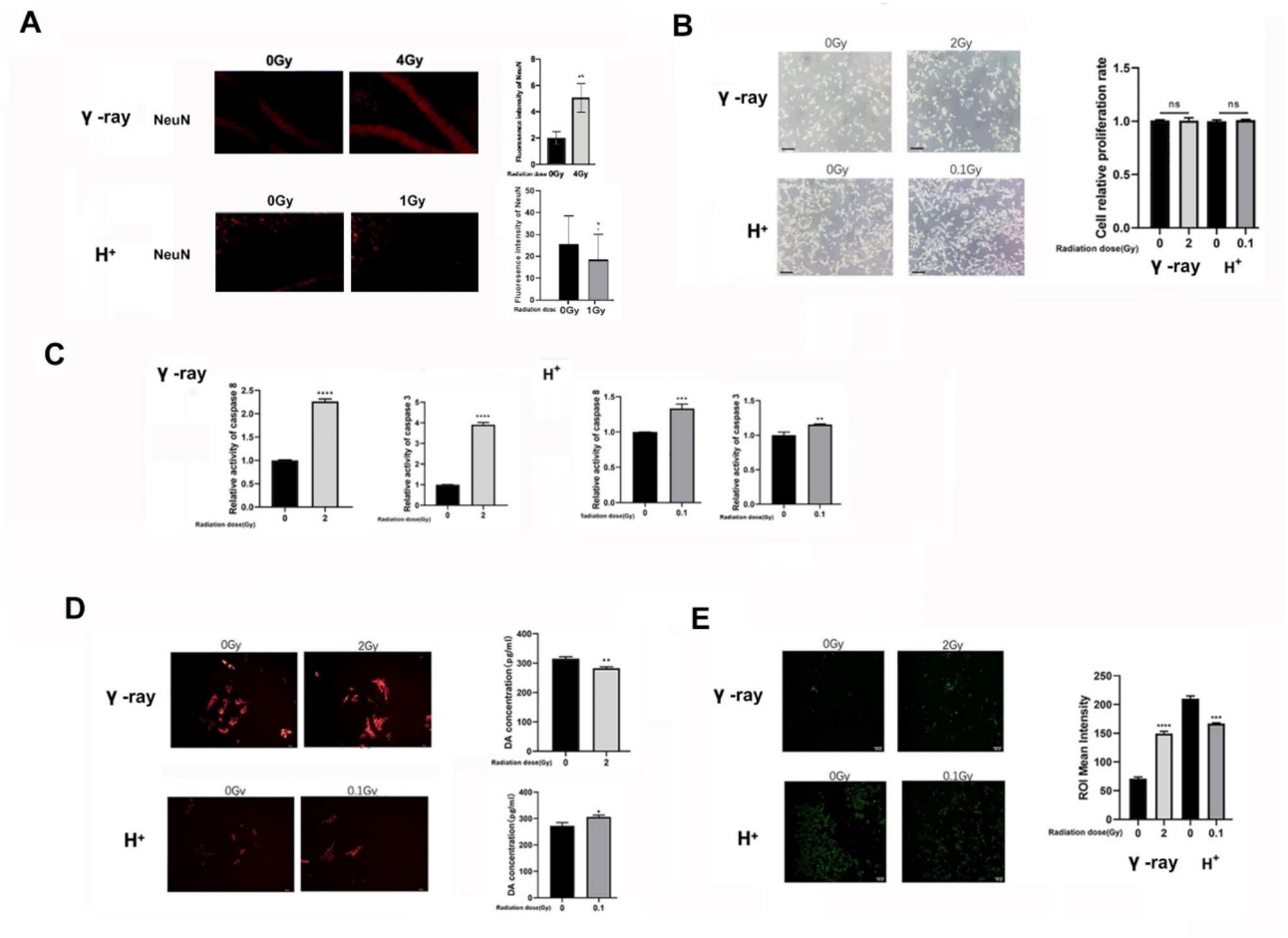

Fig. 4. Impact of irradiated astrocytes on the viability of neuronal cells. (**A**) Immunofluorescence staining of NeuN in neurons neuronal cells of the rat brain after gamma and proton beam irradiation, respectively. The magnification is 20X. (**B**) Cell proliferation rate of SH-SY5Y cells after incubated with the conditioned medium of irradiated U87 MG cells. (**C**) Caspase-3 and caspase-8 activity in SH-SY5Y cells after incubated with the conditioned medium of irradiated U87 MG cells. (**D**) Mitochondrial membrane potential and dopamine concentration in SH-SY5Y cells after incubated with the conditioned medium of irradiated U87 MG cells. The magnification is 20X.E: Glucose uptake levels in SH-SY5Y cells after incubated with the conditioned medium of irradiated U87 MG cells. $^{*}P<0.05$, $^{**}P<0.01$, $^{***}P<0.001$. γ-ray: gamma irradiation; H^{+}: proton beam irradiation; DA: dopamine.

irradiation astrocytes in the conditioned media co-cultured with neurons exhibited filamentous fragmentation of mitochondria. Gamma rays and protons at tolerated doses did not display a significant increase in mitochondrial fragmentation compared to the control group. Consequently, it can be inferred that post-irradiation astrocyte-conditioned media cultivation results in mitochondrial damage in neurons and the changes in dopamine levels in co-cultured neuronal cells also indicate that damage to neuronal mitochondria can affect dopamine metabolism levels (Fig. 4D). Moreover, considering the essential role of glucose metabolism in neuronal function, the glucose uptake levels in conditioned SH-SY5Y cells were examined. The results demonstrated that conditioning media with protons exhibited significantly decreased fluorescence intensity of glucose metabolism levels in neurons, while gamma rays showed a significant increase compared to the control group (Fig. 4E). Subsequently, we conducted a comprehensive analysis of the changes in neuronal activity and function-related indicators after culturing neurons in different radiation-induced neuroglial cell damage-conditioned media under the same tolerable dose (Table 2). Our findings revealed significant variations in the indirect effects of irradiated glial cells on neurons, shedding light on the substantial impact of post-irradiation astrocytes on mitochondrial integrity, neurotransmitter levels, and glucose metabolism in neurons.

Role of miRNAs in modulating inflammatory response to radiation

In order to investigate the impact of radiation on inflammation at the molecular level, we assessed the expression levels of GFAP and IL-6 after overexpressing miR92a-3p, miR26a-5p, and miR25-3p, which might regulate astrocyte related inflammation. It was found that miR92a-3p and miR26a-5p significantly downregulated GFAP expression, while miR25-3p overexpression led to a slightly downregulated of GFAP levels in astrocyte (Fig. 5A). Additionally, miR92a-3p overexpression significantly downregulated IL-6 expression, while miR25-3p and miR26a-5p slightly downregulated IL-6 expression without significant differences (Fig. 5A). Interestingly, gamma rays were found to significantly downregulate the expression of miR92a-3p and miR25-3p, while leaving miR26a-5p levels unchanged (Fig. 5B). Conversely, proton irradiation resulted in a significant upregulation of miR92a-3p, miR25-3p, and miR26a-5p expression levels (Fig. 5B). These findings indicated that electromagnetic radiation (gamma rays) and particle radiation (proton) may have opposite inflammatory effects on animals and cells, possibly influenced by the regulatory functions of miRNAs in astrocytes.

Discussion

In this study, our results unraveled the complexities of neuroinflammation in the context of radiation exposure. Radiation exposure induced the proliferation of astrocytes, which in turn leads to the production of inflammatory and chemotactic factors, ultimately resulting in potential neuroinflammatory damage[19]. Our research has demonstrated the inhibitory effects of various radiation types on the viability and proliferation of U87-MG cells, with higher doses leading to greater inhibition. Additionally, the upregulation of caspase-8 and caspase-3 after exposure to gamma rays suggests the potential occurrence of apoptosis in irradiated cells. These findings collectively indicated the critical impact of radiation on neuroinflammatory processes and cell viability.

GFAP, known as glial fibrillary acidic protein, is a biomarker for inflammation in the central nervous system, predominantly expressed in astrocytes. Consistently, our results also suggested that it upregulated in U87-MG cells following exposure to gamma rays, indicating widespread cellular activation[20]. In contrast, proton irradiation significantly suppressed cellular activation. IL-6, a cytokine predominantly synthesized during inflammation, plays a crucial role in activation of astrocytes[21]. Additionally, mRNA level of IL-6 was found increased in mouse microglial cells cultured with irradiation[20]. In the current study, we found an enhanced expression of IL-6, suggesting the potential promotion of neuroinflammatory reactions subsequent to radiation exposure. It is noteworthy that electromagnetic radiation induced both A1 and A2 activation in U87-MG cells, while particle irradiation did not induce activation or polarization. On this basis, we speculated that electromagnetic radiation in the radiotherapy can stimulate astrocyte activation, thereby leading to the release of pro-inflammatory factors, disruption of the central nervous immune microenvironment, and exacerbation of neuroinflammatory damage.

Astrocytes have been reported to play a crucial role in mitigating the excessive-glutamate-caused excitotoxicity by taking up excess glutamate and converting it to glutamine[22]. It was also discovered that astrocyte-mediated inflammation can be triggered by an excess of extracellular glutamate[23]. Moreover, radiation exposure could induce drops in excitatory synaptic signaling, thereby disrupting critical cognitive processes[17,24]. Notably, distinct variations were observed in the glutamine content following proton beam irradiation. In line with previous study, our findings further indicated varied effects of different radiation types on astrocyte, which imply complex indirect consequences of radiation-induced biological damage[11].

Glial cells are intricately involved in the regulation of normal central nervous system function and response to injury or stress. When astrocytes undergo a transition to a pro-inflammatory state, their ability to support neuronal survival, growth, synaptogenesis, and phagocytosis is compromised, leading to increased synaptic

Ray type and characteristic			Inhibit cell proliferation	Apoptosis Associated enzyme activity	Mitochondrial damage	Dopamine content (intracellular)	Sugar intake levels
γ-ray	Hertzian waves	Low LET low energy	–	↑	–	↓	↑
H +	particulate	Low LET medium energy	–	↑	–	↑	↓

Table 2. Effect of conditioned medium for glial cell injury induced by different radiation irradiation on neuronal activity. +: Exists, –: No change, ↑: Enhanced, ↓: Decreased.

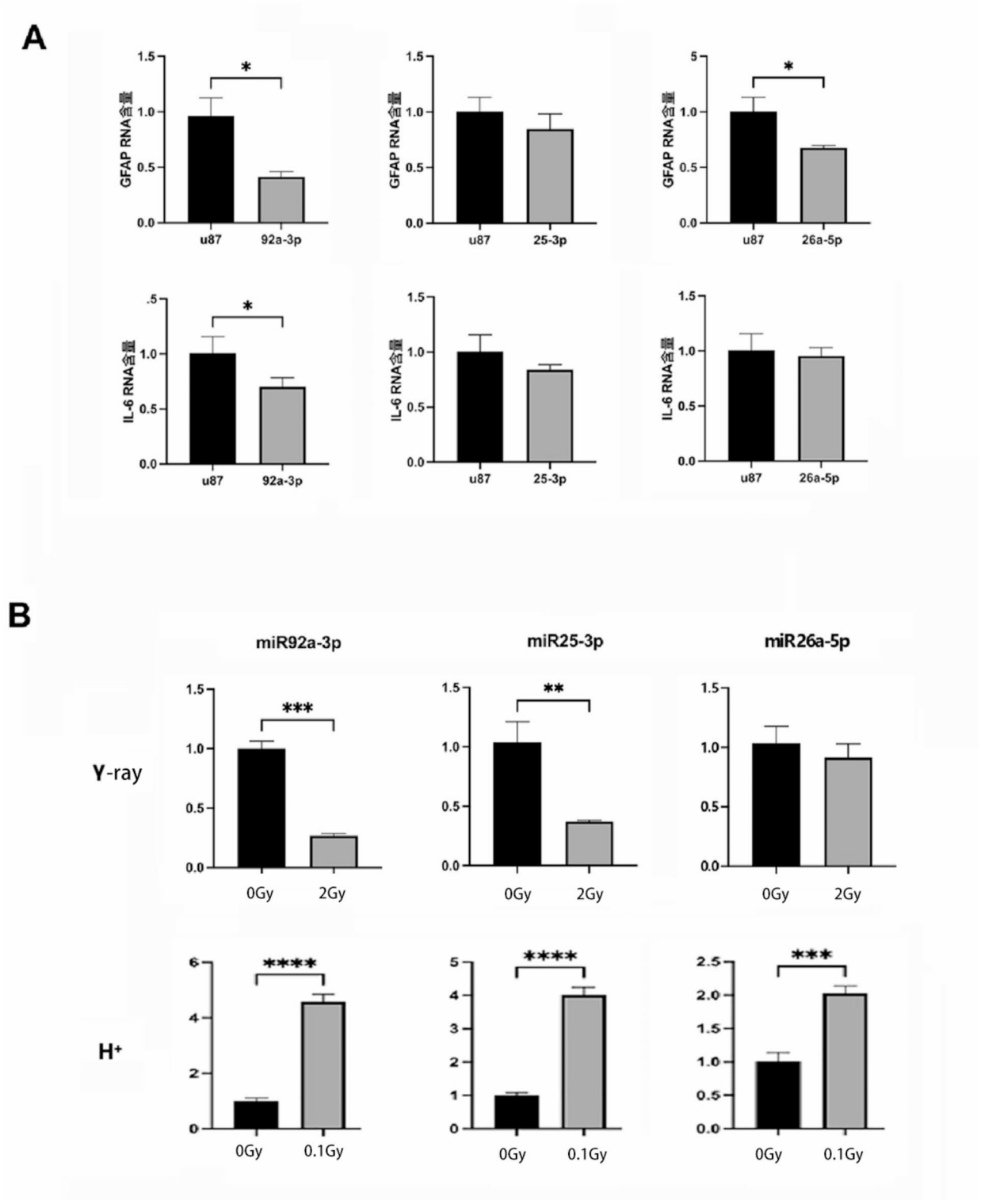

Fig. 5. Role of miRNAs in regulating radiation-induced inflammatory response of astrocytes. (**A**) Expression levels of GFAP and IL-6 in U87 MG cells after overexpressing miR92a-3p, miR26a-5p, and miR25-3p. (**B**) Expression levels of miR92a-3p, miR26a-5p, and miR25-3p in U87 MG cells after gamma and proton beam irradiation, respectively. $^{*}P<0.05$, $^{**}P<0.01$, $^{***}P<0.001$, $^{****}P<0.0001$. γ-ray: gamma irradiation; H^{+}: proton beam irradiation.

degeneration and the subsequent death of neurons and oligodendrocytes[25]. In this study, we further investigated the impact of irradiated astrocytes on neuronal cells by exposing neurons to the conditioned medium from irradiated astrocytes. Remarkably, we observed that gamma rays had a significant effect on neuronal proliferation and apoptosis, whereas proton irradiation led to distinct alterations in apoptosis-related enzymatic activity. It is important to note that mitochondria play a pivotal role in intracellular energy generation and are involved in key metabolic processes such as apoptosis, reactive oxygen species production, and lipid metabolism. Neuronal development heavily relies on functional mitochondria, and their complex morphology and high energy metabolism requirements render neurons particularly susceptible to mitochondrial dysfunction[26]. Additionally, radiation was found to diminish synaptophysin expression, lower dendritic spine number and density, and affect neurotransmitter transmission[24,27]. Notably, mitochondrial oxidative stress leads to an excessive release of dopamine, which can have detrimental effects on dopamine neurons[28,29]. It has been indicated that glutamine can promote dopamine release, whereas glutamate can enhance neuronal uptake of glucose and glycolytic activity[30]. However, excessive dopamine levels may hinder the protective effects of astrocytes on neurons, potentially leading to neuronal damage[31,32]. Our findings demonstrated that culturing neurons in post-irradiation astrocyte-conditioned media results in mitochondrial damage and substantial changes in dopamine levels and glucose metabolism. Consequently, we hypothesized that, as shown in Fig. 6, different radiation modalities may affect the glutamine content in astrocytes, thereby altering the levels of glutamine in the astrocyte-neuron microenvironment, resulting in effects on neuronal proliferation, apoptosis-related enzyme activity, mitochondrial damage, and glucose uptake levels. Nevertheless, the intricate biological effects of TME as well as the specific pro-inflammatory mechanisms by which radiotherapy affect long-term neural dysfunctions still require further investigation.

MicroRNAs (miRNAs) are pivotal in modulating inflammatory responses triggered by radiation exposure[33–35]. MicroRNAs (miRNAs) are pivotal in modulating inflammatory responses triggered by radiation exposure[36,37]. Understanding the intricate interplay between miRNAs, inflammation, and RBI is essential for developing strategies to mitigate inflammatory responses and safeguard the health of individuals exposed to the radiation environment. Certain miRNAs have been implicated in regulating the expression of pro-inflammatory cytokines and chemokines following radiation exposure. For instance, miR-223-3p has been shown to decrease the levels of proinflammatory factors, leading to a reduction in apoptosis in irradiated murine macrophages[38]. Our findings demonstrated that miR92a-3p and miR26a-5p notably downregulated GFAP expression, with miR92a-3p also significantly reducing IL-6 expression. Additionally, studies indicate that radiation exposure can alter miRNA expression profiles, subsequently impacting inflammatory responses[39]. In this study, we found that gamma rays significantly decreased the expression of miR92a-3p and miR25-3p, while proton irradiation led to a marked increase in the levels of miR92a-3p, miR25-3p, and miR26a-5p. The findings underscored the critical role of miRNAs in modulating inflammatory responses to radiation exposure. However, further exploration is warranted to elucidate the specific mechanisms through which these miRNAs regulate inflammatory pathways in response to two types of radiation exposure (Fig. 6).

Experiments have shown that cells that have not been directly irradiated can also be affected when cultured in a medium that receives directly irradiated cells. Radiation therapy is an important method for cancer. Different organizations have different sensitivities to radiation therapy. Therefore, the therapeutic effects also vary. In the comprehensive treatment of tumors, it is necessary to decide which diseases can be treated with radiation therapy as an adjuvant therapy. The non-targeted effects of ionizing radiation may have a certain impact on the efficacy of radiotherapy. Shao et al.[40] used microbeam helium ions to treat T98G glial cells, a small portion of the tumor cell population was precisely irradiated, and the results showed that not only has there been an increase in lethal damage to nearby tumor cells that have not been irradiated, but also normal surrounding cells are also significantly damaged. It can be seen that radiation-induced non-targeted side effects have an impact on cells. Therefore, during radiotherapy, it is required to make appropriate adjustments to the radiation biological dose damage model and protection methods, design the irradiation target area and dose distribution more reasonably, and carry out more accurate radiotherapy techniques. Precise treatment may still result in low-dose irradiation of organs near the tumor, and non- irradiated tissues and cells around the tumor are inevitably at risk of radiation bystander effects[41–43]. In addition, the elucidation of the formation mechanism of non -target effects induced by radiation may provide new impetus for the study of accompanying effects found in patients during or after radiation therapy, helping to explain the accompanying effects of radiation therapy in patients, such as headaches, joint pain and so on. At present, the anti-inflammatory effect of radiotherapy has been widely used in patients with benign joint diseases, but its mechanism is not fully understood. Many studies suggest that non-targeted effects, side effects, and inflammation may have similar formation and transformation mechanisms[44,45].

There are many factors that affect cell proliferation, including apoptosis. Numerous studies have shown that one of the biological effects of radiation is that it can cause apoptosis in various cells, including nerve cells. By detecting the strength of Caspase-3 activity, the degree of cell apoptosis can be determined[46]. Normal mitochondrial membrane potential is a prerequisite for maintaining mitochondrial oxidative phosphorylation and ATP production, and is necessary for maintaining mitochondrial function. The decrease in mitochondrial membrane potential is a hallmark event in the early stage of cell apoptosis.

In our study, it was observed that gamma irradiation of glial cells can induce a decrease in neuronal mitochondrial membrane potential in their culture medium, which is consistent with the occurrence of cell apoptosis and an increase in caspase-3 activation levels. In the proton irradiation experiment, we speculate that there is a non-caspase-3 dependent neuronal effect, which corresponds to the absence of significant changes in neuronal mitochondria. We will conduct further exploration in the future to reveal the damage mechanism of proton radiation-induced glial cell immune imbalance to neurons.

In summary, the study demonstrated that gamma rays and proton radiation have differential impacts on inflammatory responses in vivo and astrocyte viability. Gamma rays induced a pro-inflammatory effect, while

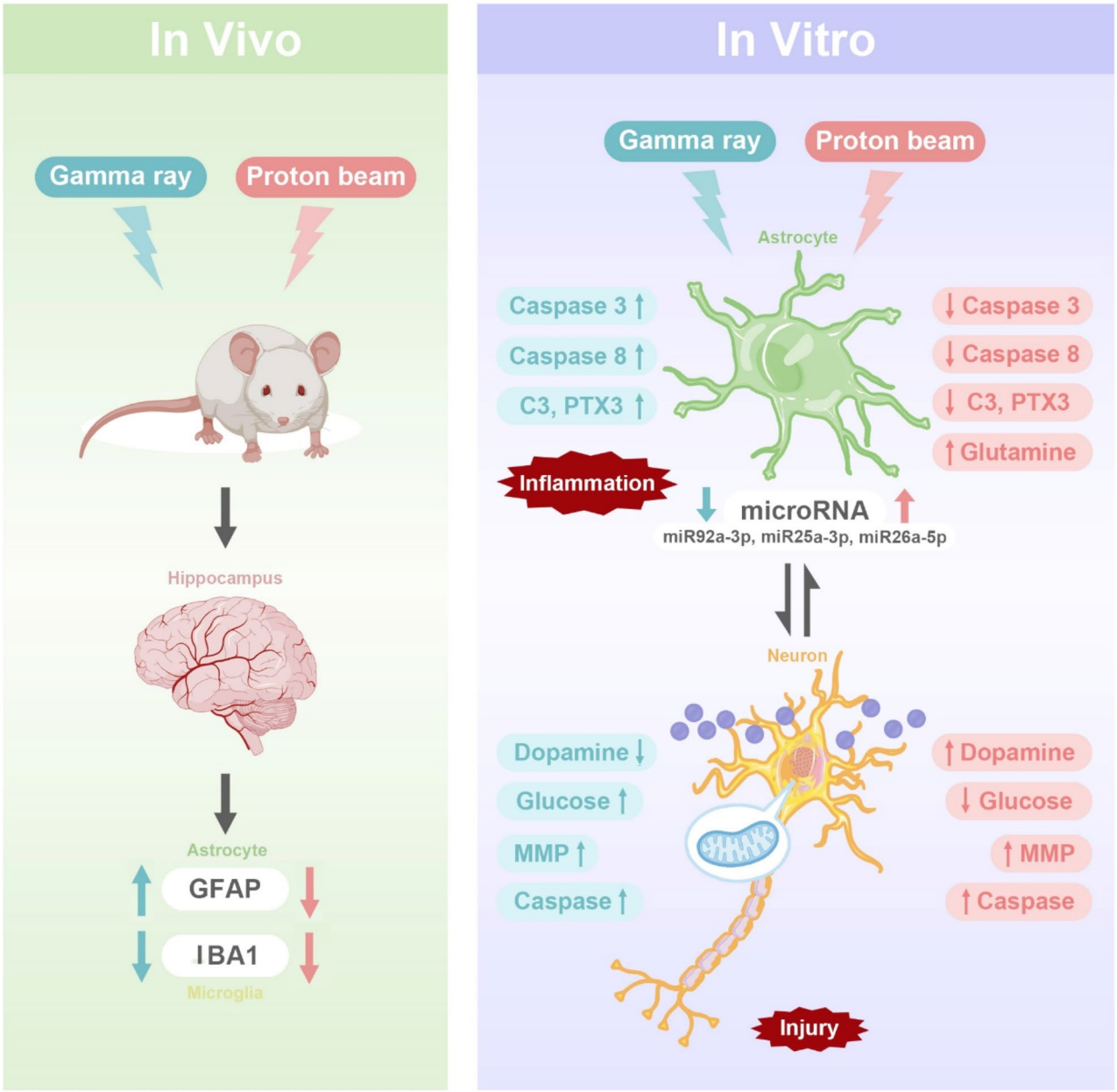

Fig. 6. Distinct astrocyte activation patterns associated with neuroinflammation induced by Gamma and proton beam irradiation. Gamma and proton beam irradiation induced distinct astrocyte activation patterns associated with neuroinflammation. Furthermore, gamma radiation affected co-cultured neurons and astrocytes by disrupting mitochondrial integrity, altering DA expression levels, and influencing glucose metabolism. While gamma radiation triggered pro-inflammatory effects, proton beam irradiation may elicit anti-inflammatory responses, with miR92a-3p potentially serving as a crucial factor in modulating the divergent activities.

proton radiation exhibited anti-inflammatory properties. Two types of radiation also influenced enzyme activity, gene expression, glutamine levels, and cellular metabolism in astrocytes, affecting neuronal activity. Moreover, miRNAs played a role in modulating the inflammatory response to radiation. The findings have implications for understanding the potential mechanisms underlying various radiation-induced inflammatory and offer insights for future protective or adjuvant therapy strategies.

Data availability

The datasets used and/or analyzed during the current study are available from the corresponding author on reasonable request.

Received: 23 September 2024; Accepted: 17 March 2025
Published online: 03 April 2025

References

1. Ali, F. S. et al. Cerebral radiation necrosis: Incidence, pathogenesis, diagnostic challenges, and future opportunities. *Curr. Oncol. Rep.* **21**(8), 66 (2019).
2. Brown, P. D. et al. Effect of radiosurgery alone vs radiosurgery with whole brain radiation therapy on cognitive function in patients with 1 to 3 brain metastases: A randomized clinical trial. *JAMA* **316**(4), 401–409 (2016).
3. Hladik, D. & Tapio, S. Effects of ionizing radiation on the mammalian brain. *Mutat. Res. Rev. Mutat. Res.* **770**(Pt B), 219–230 (2016).
4. Balentova, S. & Adamkov, M. Pathological changes in the central nervous system following exposure to ionizing radiation. *Physiol. Res.* **69**(3), 389–404 (2020).
5. Rahman, R., Alexander, B. M. & Wen, P. Y. Neurologic complications of cranial radiation therapy and strategies to prevent or reduce radiation toxicity. *Curr. Neurol. Neurosci. Rep.* **20**(8), 34 (2020).
6. Chen, Z. et al. Altered expression of inflammation-associated molecules in striatum: An implication for sensitivity to heavy ion radiations. *Front. Cell Neurosci.* **17**, 1252958 (2023).
7. Ma, H. et al. Transcriptome analysis of glioma cells for the dynamic response to gamma-irradiation and dual regulation of apoptosis genes: A new insight into radiotherapy for glioblastomas. *Cell Death Dis.* **4**(10), e895 (2013).
8. Monjazeb, A. M. et al. Effects of radiation on the tumor microenvironment. *Semin. Radiat. Oncol.* **30**(2), 145–157 (2020).
9. Nagane, M., Yasui, H., Kuppusamy, P., Yamashita, T. & Inanami, O. DNA damage response in vascular endothelial senescence: Implication for radiation-induced cardiovascular diseases. *J. Radiat. Res.* **62**(4), 564–573 (2021).
10. Marretta, A. L. et al. Response to peptide receptor radionuclide therapy in pheocromocytomas and paragangliomas: A systematic review and meta-analysis. *J. Clin. Med.* **12**(4), 1494 (2023).
11. Rahman, R. et al. DNA damage response in brain tumors: A Society for Neuro-Oncology consensus review on mechanisms and translational efforts in neuro-oncology. *Neuro. Oncol.* **26**(8), 1367–1387 (2024).
12. Liu, G. et al. Ferulic acid produces neuroprotection against radiation-induced neuroinflammation by affecting NLRP3 inflammasome activation. *Int. J. Radiat. Biol.* **98**(9), 1442–1451 (2022).
13. Jacob, J. et al. Cognitive impairment and morphological changes after radiation therapy in brain tumors: A review. *Radiother. Oncol.* **128**(2), 221–228 (2018).
14. Colangelo, N. W. & Azzam, E. I. Extracellular vesicles originating from glioblastoma cells increase metalloproteinase release by astrocytes: The role of CD147 (EMMPRIN) and ionizing radiation. *Cell Commun. Signal* **18**(1), 21 (2020).
15. Tang, F. R., Liu, L., Wang, H., Ho, K. J. N. & Sethi, G. Spatiotemporal dynamics of gammaH2AX in the mouse brain after acute irradiation at different postnatal days with special reference to the dentate gyrus of the hippocampus. *Aging (Albany NY)* **13**(12), 15815–15832 (2021).
16. Kumar, G., Dutta, P., Parihar, V. K., Chamallamudi, M. R. & Kumar, N. Radiotherapy and its impact on the nervous system of cancer survivors. *CNS Neurol. Disord. Drug Targets* **19**(5), 374–385 (2020).
17. Yan, L. et al. The biological implication of semicarbazide-sensitive amine oxidase (SSAO) Upregulation in rat systemic inflammatory response under simulated aerospace environment. *Int. J. Mol. Sci.* **24**(4), 3666 (2023).
18. Lee, H. G., Wheeler, M. A. & Quintana, F. J. Function and therapeutic value of astrocytes in neurological diseases. *Nat. Rev. Drug. Discov.* **21**(5), 339–358 (2022).
19. Turnquist, C. et al. Radiation-induced astrocyte senescence is rescued by Delta133p53. *Neuro. Oncol.* **21**(4), 474–485 (2019).
20. Hwang, S. Y. et al. Ionizing radiation induces astrocyte gliosis through microglia activation. *Neurobiol. Dis.* **21**(3), 457–467 (2006).
21. Li, D. et al. NK cell-derived exosomes carry miR-207 and alleviate depression-like symptoms in mice. *J. Neuroinflamm.* **17**(1), 126 (2020).
22. Sonnay, S. et al. Astrocytic and neuronal oxidative metabolism are coupled to the rate of glutamate-glutamine cycle in the tree shrew visual cortex. *Glia* **66**(3), 477–491 (2018).
23. Limon, I. D., Angulo-Cruz, I., Sanchez-Abdon, L. & Patricio-Martinez, A. Disturbance of the glutamate-glutamine cycle, secondary to hepatic damage, compromises memory function. *Front. Neurosci.* **15**, 578922 (2021).
24. Alaghband, Y. et al. Galactic cosmic radiation exposure causes multifaceted neurocognitive impairments. *Cell Mol. Life Sci.* **80**(1), 29 (2023).
25. Martinez, A. et al. Characterization of microglia behaviour in healthy and pathological conditions with image analysis tools. *Open Biol.* **13**(1), 220200 (2023).
26. Sweetat, S. et al. The beneficial effect of mitochondrial transfer therapy in 5XFAD mice via liver-serum-brain response. *Cells* **12**(7), 1006 (2023).
27. Parihar, V. K. et al. Cosmic radiation exposure and persistent cognitive dysfunction. *Sci. Rep.* **6**, 34774 (2016).
28. Chen, C. et al. Dexmedetomidine can enhance PINK1/parkin-mediated mitophagy in MPTP-induced PD mice model by activating AMPK. *Oxid. Med. Cell Longev.* **2022**, 7511393 (2022).
29. Burbulla, L. F. et al. Dopamine oxidation mediates mitochondrial and lysosomal dysfunction in Parkinson's disease. *Science* **357**(6357), 1255–1261 (2017).
30. Oya, M. et al. Increased glutamate and glutamine levels and their relationship to astrocytes and dopaminergic transmissions in the brains of adults with autism. *Sci. Rep.* **13**(1), 11655 (2023).
31. Masato, A., Bubacco, L. & Greggio, E. Too much for your own good: Excessive dopamine damages neurons and contributes to Parkinson's disease: An Editorial Highlight for "Enhanced tyrosine hydroxylase activity induces oxidative stress, causes accumulation of autotoxic catecholamine metabolites, and augments amphetamine effects in vivo". *J. Neurochem.* **158**(4), 833–836 (2021).
32. Mitsuyo, T. et al. Facilitation of ischemia-induced release of dopamine and neuronal damage by dexamethasone in the rat striatum. *Eur. J. Pharmacol.* **465**(3), 267–274 (2003).
33. Yang, L. et al. Mesenchymal stem cell-derived exosomes are effective for radiation enteritis and essential for the proliferation and differentiation of Lgr5(+) intestinal epithelial stem cells by regulating Mir-195/Akt/beta-catenin pathway. *Tissue Eng. Regen. Med.* **20**(5), 739–751 (2023).
34. Csordas, I. B. et al. The miRNA content of bone marrow-derived extracellular vesicles contributes to protein pathway alterations involved in ionising radiation-induced bystander responses. *Int. J. Mol. Sci.* **24**(10), 8607 (2023).
35. Choi, Y. Y. et al. The miR-126-5p and miR-212-3p in the extracellular vesicles activate monocytes in the early stage of radiation-induced vascular inflammation implicated in atherosclerosis. *J. Extracell. Vesicles* **12**(5), e12325 (2023).
36. Chan, Y. H., Wang, C., Soh, W. K. & Rajapakse, J. C. Combining neuroimaging and omics datasets for disease classification using graph neural networks. *Front. Neurosci.* **16**, 866666 (2022).
37. Xu, P., Xu, H., Cheng, H. S., Chan, H. H. & Wang, R. Y. L. MicroRNA 876–5p modulates EV-A71 replication through downregulation of host antiviral factors. *Virol. J.* **17**(1), 21 (2020).
38. Zhang, M. et al. MiR-223-3p attenuates radiation-induced inflammatory response and inhibits the activation of NLRP3 inflammasome in macrophages. *Int. Immunopharmacol.* **122**, 110616 (2023).

39. Fang, C. et al. microRNA-193a stimulates pancreatic cancer cell repopulation and metastasis through modulating TGF-beta2/TGF-betaRIII signalings. *J. Exp. Clin. Cancer Res.* **37**(1), 25 (2018).
40. Iyer, R. & Lehnert, B. E. Low dose, low-LET ionizing radiation-induced radioadaptation and associated early responses in unirradiated cells. *Mutat. Res.* **503**(1–2), 1–9 (2002).
41. Shao, C., Folkard, M. & Prise, K. M. Role of TGF-beta1 and nitric oxide in the bystander response of irradiated glioma cells. *Oncogene* **27**(4), 434–440 (2008).
42. Mackonis, E. C. et al. Cellular response to modulated radiation fields. *Phys. Med. Biol.* **52**(18), 5469–5482 (2007).
43. Suchowerska, N., Ebert, M. A., Zhang, M. & Jackson, M. In vitro response of tumour cells to non-uniform irradiation. *Phys. Med. Biol.* **50**(13), 3041–3051 (2005).
44. Camphausen, K. et al. Radiation abscopal antitumor effect is mediated through p53. *Cancer Res.* **63**(8), 1990–1993 (2003).
45. Mothersill, C. & Seymour, C. Radiation-induced bystander effects: Past history and future directions. *Radiat. Res.* **155**(6), 759–767 (2001).
46. Elmore, S. Apoptosis: A review of programmed cell death. *Toxicol. Pathol.* **35**(4), 495–516 (2007).

Author contributions

H M conceived the experiments; LB Y, TY E, A W and BQ L performed the experiments; SQ S and H M wrote the manuscript;H M, ZR W and J Z secured funding; YL D, QJ W and L S provided irradiation conditions. SQ S and H M contributed to the drafting of the article and final approval of the submitted version.

Funding

This work was supported by grants from space Medical Experiment Project of China Manned Space Program (No. HYZHXM02003) to Hong Ma, and Science Foundation of Aerospace Medical & Healthcare Technology Corporation (AMHT, Grant NO. 2023YK05) to Hong Ma and Shaoqian Sun.

Declarations

Competing interests

The authors declare no competing interests.

Additional information

Correspondence and requests for materials should be addressed to S.S., L.S. or H.M.

Reprints and permissions information is available at www.nature.com/reprints.

Publisher's note Springer Nature remains neutral with regard to jurisdictional claims in published maps and institutional affiliations.